Published in final edited form as:
J Immunol. 2010 February 15; 184(4): 1858–1866. doi:10.4049/jimmunol.0903210.

IL-12 Suppresses Vascular Endothelial Growth Factor Receptor 3 Expression on Tumor Vessels by Two Distinct IFN-γ–Dependent Mechanisms

Elizabeth W. Sorensen, **Scott A. Gerber**, **John G. Frelinger**, and **Edith M. Lord**
Department of Microbiology and Immunology, University of Rochester Medical Center, Rochester, NY 14642

Abstract

IL-12 has been shown to be effective in enhancing antitumor responses. However, how IL-12 exerts its antiangiogenic effect is largely unknown. In this study, we elucidate this mechanism using B16 transfected to express IL-12 (B16/IL-12), a system that provides constant, local production of IL-12 within the tumor microenvironment. Intratumoral IL-12 resulted in a significant delay in tumor growth and phenotypic changes in the vasculature. Vessels found within B16 tumors are chaotic and poorly formed and express vascular endothelial growth factor receptor 3 (VEGFR3), a growth factor receptor not expressed on normal adult vessels. However, the vessels within B16/IL-12 tumors have a more normal morphology and do not express VEGFR3. We have shown that IFN-γ is required for IL-12 to suppress the aberrant expression of VEGFR3. Indeed, the presence of intratumoral IL-12 stimulates the immune system resulting in more IFN-γ–producing tumor-infiltrating lymphocytes per tumor when compared with parental B16 tumors, which may have a marked effect on control of tumor growth. Interestingly, within B16/IL-12 tumors, T cells are necessary to suppress VEGFR3 expression on tumor vessels. Finally, using IFN-γ receptor knockout mice in a bone marrow chimera system, we show that the IFN-γ produced within the tumor suppresses VEGFR3 expression in two ways: 1) acting directly on tumor vessel endothelial cells, and 2) acting on the tumor-infiltrating lymphocytes to indirectly alter endothelial cells' VEGFR3 expression. Our data indicate a mechanism in which tumor-infiltrating immune cells regulate tumor vessel phenotype.

Targeting the immune system to treat cancer has long been an important goal of cancer therapy; however, achieving this goal has been hindered by our limited understanding of the exact cellular and molecular mechanisms underlying the immune/tumor microenvironment interactions. For instance, cytokine-based strategies have included i.v. injection of immunomodulatory cytokines such as IL-12, IL-2, IFN-α, and IFN-γ, alone or in combination. The success of such strategies has been limited by the short half-life of circulating cytokines and side effects associated with their use in higher concentrations (1-3).

IL-12, a cytokine that plays an important role in both innate and adaptive immune responses, acts on both cytotoxic T cells and NK cells (4,5) and is one of the main cytokines involved in eliciting type I T cell responses in the form of both $CD4^+$ Th1 cells and $CD8^+$ Tc1 cells

Address correspondence and reprint requests to Dr. Edith M. Lord, Department of Microbiology and Immunology, Box 672, 601 Elmwood Avenue, Rochester, NY 14642. Edith_Lord@urmc.rochester.edu .

Disclosures The authors have no financial conflicts of interest.

(6,7). In addition, it has been shown to have significant stimulatory effects on the host antitumor immune response by stimulating tumor-infiltrating lymphocytes (TILs) to produce IFN-γ (8-10). Although the systemic delivery of IL-12 has been effective in enhancing antitumor responses in metastatic melanoma and renal cell carcinoma, severe side effects in clinical trials have limited its application (11-13).

To gain better understanding of the role of IL-12 within the tumor microenvironment, we and others have investigated its antitumor effects in multiple preclinical animal models of melanoma, and demonstrated that IL-12 not only enhances the infiltration and function of host immune cells, but surprisingly, suppresses the development of new blood vessels as well, a process termed angiogenesis (14-17). Angiogenesis is a complex process affected by many different factors. In normal tissue, the vast majority of vessels are quiescent and the same is true for very small tumors that are oxygenated through diffusion from existing surrounding vessels. However, as tumors grow and become hypoxic, the tumor cells secrete large amounts of proangiogenic growth factors that, in the absence of opposing antiangiogenic factors, cause uncontrolled vessel growth and promote tumor progression. The tumor vessels are typically large, poorly formed, and leaky, either having an overabundance or complete lack of basement membrane (18). It has been postulated that some anti-angiogenic therapies may actually normalize these vessels, which has been defined as the pruning of excess vessels, leading to the formation of a more efficient vascular network. This may allow better delivery of chemotherapeutic agents, Ab treatments, and host immune cells (18,19).

To elucidate the effects in vivo of IL-12, we developed an IL-12–producing B16 melanoma tumor cell line (B16/IL-12), which provides local delivery of IL-12 and enables the experimental study of the immunological and vascular effects of IL-12 within the tumor microenvironment. Our previous studies have demonstrated that in addition to delayed growth kinetics, B16/IL-12 elicits profound morphological changes in the vasculature along with the suppression of the proangiogenic receptor, vascular endothelial growth factor receptor 3 (VEGFR3), on the tumor vessels (20).

Tumor angiogenesis is regulated by multiple receptors expressed on blood vessel endothelial cells. VEGFR3, one of the three receptors that bind members of the proangiogenic vascular endothelial growth factor (VEGF) family, is typically expressed only on embryonic blood vessels and adult lymphatic vessels (21,22). Although downregulated on quiescent adult vessels, it can be upregulated during angiogenesis, either in the context of chronic wound healing (23), or within growing tumors (24-27). Using Abs to block VEGFR3 on tumor vessels can lead to an inhibition of tumor angiogenesis (28,29). The main ligand for VEGFR3, VEGF-C, is known to affect lymphangiogenesis in multiple models; however, its effects on angiogenesis are controversial and may be dependent on the specific tumor model (30-32). The mechanism through which VEGFR3 is regulated on both normal and tumor vessels is poorly understood. However, recent reports have begun to shed light on this process. For example, VEGF-A injected into monkey eyes induced VEGFR3 on both existing vessels and on angiogenic vascular sprouts thereby promoting angiogenesis (33). Alternatively, Notch1 can suppress VEGFR3 on the surface of vessels, as evidenced by the use of pharmacological inhibitors of Notch signaling causing an upregulation of VEGFR3 expression on blood vessel endothelial cells (34). In our current study, we elucidate how the interplay via stimulation of cytokine production between TILs, specifically T cells, and tumor vessel endothelial cells is required to induce the suppression of VEGFR3 on tumor vessels. In particular, we demonstrate that IFN-γ can act both directly on the tumor vessels and indirectly through immune cells to suppress VEGFR3 expression within B16/IL-12 tumors.

Materials and Methods

Mice and cell lines

C57BL/6Jwild-type(WT), B6.129S7-*Ifng*^{tm1ts}(IFN-γ–deficient), B6.129S7-*Ifngr1*^{tm1Agt}/J (IFN-γ receptor-deficient), and B6.129P2-*Cxcr3*^{tm1Dgen}/J (CXCR3-deficient) mice were purchased from The Jackson Laboratory (Bar Harbor, ME). Nude mice were purchased from Taconic Farms (Germantown, NY). GFP-transgenic mice (C57BL/6-H-2KbP-GFP) were generated as previously described (35). B6.129S1-*Il12rb2*^{tm1Jm}/J (IL-12 receptor β2-chain–deficient) mice were a kind gift from B. Segal (University of Rochester, Rochester, NY). The transgenic mice were bred in the animal facility at the University of Rochester. Guidelines for the humane treatment of animals were followed, as approved by the University Committee on Animal Resources. The B16-F0 (B16) cell line, a spontaneously arising C57BL/6-derived melanoma, was obtained from the American Type Culture Commission (Manassas, VA; CRL 6322). B16-F0 transfected to express IL-12p70 (B16/IL-12) has been previously described (20). Tumor cell lines were maintained in MAT/P medium (U.S. patent 4.816.401) supplemented with 100 U/ml penicillin, 100 mg/ml streptomycin, and 2% FCS. In addition, 400 mg/ml G418 (Life Technologies, Rockville, MD) was added to the medium used to culture B16/IL-12.

Tumor growth

Tumor cells (2×10^5) were injected in 100 μl HBSS (Sigma-Aldrich, St. Louis, MO) i.m. into the thigh muscle of the mice. Mean thigh diameters were determined, as described previously (36). Mice were sacrificed when the mean thigh diameter reached 10–13 mm.

Whole mount histology and image analysis

Tumor vasculature analysis was performed as previously described (20). In brief, small pieces of tumor were excised and stained at 4°C in staining buffer (PBS and 1% BSA, 0.1% sodium azide). Samples were blocked using Fc Block (BD Pharmingen, San Diego, CA) and the primary Abs, allophycocyanin-conjugated anti-CD31 (BD Pharmingen) and biotinylated anti-VEGFR3 (R&D Systems, Minneapolis, MN) added directly to the tube at predetermined concentrations. The samples were then incubated at 4°C with rocking for 2 h. The samples were then washed once in staining buffer, streptavidin-PE (BD Pharmingen) added at a dilution of 1:1000 in staining buffer and stained for an additional hour as described previously. Stained tumor samples were then viewed using a fluorescence microscope connected to a monochrome CCD digital camera. Band-pass filter cubes designed to detect allophycocyanin and PE wavelengths were used to acquire alternate images of the same fields of view. Monochrome images were analyzed using ImagePro Plus software (MediaCybernetics, Bethesda, MD). The percentage area of VEGFR3 positive tumor vessels was determined by first autothresholding the CD31 image, based on pixel intensity, to construct a binary mask. The corresponding VEGFR3 image was thresholded in the same way, and the masked images combined to produce an image that included only the portions of the image that were positive for both CD31 and VEGFR3. The percent area of this image was then divided by the percent CD31 area to attain the proportion of tumor vessels that were VEGFR3$^+$ for that field of view.

Generation of bone marrow chimeric mice

Bone marrow was isolated from femurs of WT, IL-12Rβ2–deficient (IL-12Rβ2$^{-/-}$), and IFN-γR–deficient (IFN-γR$^{-/-}$) mice and washed twice in HBSS. Bone marrow cells (3×10^6) in HBSS were injected i.v. into lethally irradiated (10 Gy) WT, IL-12Rβ2$^{-/-}$, or IFN-γR$^{-/-}$ recipient mice on the same day. After injection, chimeric mice were allowed to rest for a minimum of 8 wk before experimental use.

Flow cytometric analysis and detection of IFN-γ–secreting cells

Tumors were minced with scissors and dissociated using collagenase as previously described (37). The single cell suspensions were cultured in MAT/P media supplemented with 5% FCS (Hyclone Laboratories, Lakewood, NJ) and 10 μg/ml Trp-2 peptide (SYVDFFVWL) for 16–18 h. GolgiPlug (BD Biosciences, San Jose, CA) was then added to the culture for 6 h. The cells were then blocked using Fc block and stained with PerCP anti-CD45 (clone 30-F11, BD Pharmingen), FITC anti-CD8 (clone 53-6.7, eBioscience, San Diego, CA), allophycocyanin anti-CD4 (clone GK1.5, eBioscience), or PE anti-NK1.1 (PK136) to identify host immune cell populations. Cells were then fixed and permeablized with 4% paraformaldehyde and stained with PE anti–IFN-γ (XMG1.2, BD Pharmingen) Samples were analyzed using a FACSCalibur flow cytometer and Cell-Quest software (BD Biosciences).

Ab depletion of NK cells

In nude mice, NK cells were depleted using a rat anti-mouse IL-2Rβ mAb (TM-β1) (38). Briefly, mice were injected with 0.5 mg/mouse Ab on days 2 and 7 after tumor injection. In C57BL/6 mice, NK cells were depleted by treating them two times per week with 100 μg/mouse and once per week with 300 μg/mouse rat anti-NK1.1 Ab (PK136).

Results

IL-12 significantly delays the growth of B16

Previously, our laboratory has shown that local, continuous production of IL-12 within the tumor microenvironment causes a delay in the growth of B16 melanoma in WT mice (20). To extend these findings and show that the mechanism of the tumor control is indeed mediated through the IL-12 receptor, we injected B16 or B16/IL-12 into both WT and IL-12Rβ2$^{-/-}$ mice. Although IL-12Rβ2$^{-/-}$ mice express the high affinity receptor for IL-12 and can bind the IL-12 heterodimer, they lack the ability to signal through it. In addition, the IL-12Rβ2–chain is the only chain of the trimeric IL-12 receptor to be exclusively specific to IL-12; both the IL-12Rα– and β1-chains are also part of the IL-23 receptor. As a result, IL-12Rβ2$^{-/-}$ mice have completely normal IL-23 binding and receptor signaling, but deficient IL-12 receptor signaling.

To compare the growth kinetics of these cell lines in both mouse strains, equivalent numbers of tumor cells were injected i.m. into the animals and thigh diameter measured over time. Consistent with our earlier findings, B16/IL-12 grew with significantly slower kinetics than the parental line (Fig. 1*A*) (20). There was no difference in the growth of these cell lines in vitro (data not shown), indicating that the differences seen in vivo were not due to clonal variation among cell lines. As expected, when B16/IL-12 was injected into IL-12Rβ2$^{-/-}$ mice, the kinetics of growth were indistinguishable from that of the parental line (Fig. 1*B*), suggesting that the tumor suppression seen in WT mice was due to the presence of IL-12. The identical kinetics of tumor growth in IL-12Rβ2$^{-/-}$ and WT mice also indicates that the effect of the IL-12 produced within the tumor is mediated through IL-12 receptor signaling on host cells and not on the tumor cells directly.

IL-12 indirectly suppresses VEGFR3 on tumor vessel endothelial cells

Using multiple staining techniques (20) we have previously shown that VEGFR3 is reduced on tumor vessels as a result of the local production of IL-12; however, the mechanism of suppression is not well understood. To examine the dependence of VEGFR3 suppression on IL-12, we performed whole mount histology on B16 and B16/IL-12 tumors grown in both C57BL/6 (WT) and IL-12Rβ2$^{-/-}$ mice. Because of the in vivo disparity in growth curves between these lines, all tumors were grown to equivalent thigh diameters before removal

and staining with anti-CD31 and anti-VEGFR3. Fig. 2 shows representative images from B16 (*upper panels*) and B16/IL-12 (*lower panels*) tumors grown in both WT (Fig. 2*A*) and IL-12Rβ2$^{-/-}$ (Fig. 2*B*) mice. Each row of images represents the same field of view using different filter sets; anti–CD31-allophycocyanin (pseudo-colored green), anti–VEGFR3-PE (pseudo-colored red), and a composite image of both. As expected, B16 tumors from both WT and IL-12Rβ2$^{-/-}$ mice stained positive for VEGFR3 in a vascular pattern. The vascular pattern of staining was not evident when B16/IL-12 was injected into WT mice. However, when B16/IL-12 was injected into IL-12Rβ2$^{-/-}$ mice, which were unable to respond to the intratumoral IL-12, there was little to no suppression of the VEGFR3 on the tumor vessels (Fig. 2*B*). The extent to which VEGFR3 was suppressed on the vessels within these tumors was calculated by determining the proportion of vessel area (CD31^{+}) that stained for VEGFR3 using the ImagePro software, as described in the *Materials and Methods* (Fig. 3*A*). We determined that viable B16 tumor cells do not express VEGFR3 in vitro or in vivo; however, necrotic tumor cells nonspecifically bind the VEGFR3 Ab (data not shown), and considerable nonspecific staining of nonvascular, necrotic cells was seen in B16/IL-12 tumors (Fig. 2*A*, *lower panels*). Previous work using the VEGFR3 Ab on thin sections has confirmed that the staining seen in B16/IL-12 is not on the vessels and any overlap seen is a result of the whole mount technique, as the figure is a projected image of multiple planes of the field of view (20). This nonspecific, nonvascular staining is represented by a dotted line in all figures that quantify VEGFR3 staining.

To determine whether IL-12 acts directly on the tumor vessel endothelial cells, we generated bone marrow chimeric mice using bone marrow from IL-12Rβ2$^{-/-}$ mice to reconstitute WT mice that were given a lethal whole-body radiation dose of 10 Gy (IL-12R$^{-/-}$→WT) and allowed to recover for a minimum of 8 wk before use. Under these conditions, although the radioresistant host cells would be able to respond to IL-12 produced within B16/IL-12, the reconstituted hematopoietic cells would not. We generated the reverse chimeras (WT→IL-12R$^{-/-}$), in which the hematopoietic cells could respond to the IL-12 produced within the tumor, but the stromal cells and vascular endothelium could not, as well as (WT→WT) and (IL-12R$^{-/-}$→IL-12R$^{-/-}$) chimeras to control for the effects of the radiation and reconstitution process. B16 and B16/IL-12 cells were injected into these mice and vascular VEGFR3 levels assessed by whole mount histology. In tumors in which the vessels had the ability to respond to the IL-12 produced locally, but the immune cells did not, the presence of IL-12 within the tumor failed to suppress the upregulation of VEGFR3 on the tumor vessels. However, the vascular expression of VEGFR3 was suppressed in the reverse chimeras (Fig. 3*B*). This indicates that the IL-12 within B16/IL-12 does not act directly on the tumor vessels, but requires WT hematopoietic cells that can respond to the IL-12 produced within the tumor. Also, the WT→WT and IL-12R$^{-/-}$→IL-12R$^{-/-}$chimeric mice yielded the same results as the nonchimeric WT and IL-12Rβ2$^{-/-}$ mice, respectively (data not shown).

IFN-γ is required to suppress VEGFR3

Because our results suggest that a downstream product of IL-12, produced by hematopoietically derived cells, is required to suppress the upregulation of VEGFR3 on tumor vasculature, we hypothesized that IFN-γ, a major product of IL-12 signaling, may have a role in the suppression of VEGFR3. To test this, B16 and B16/IL-12 were injected into IFN-γ$^{-/-}$ mice. In mice that lack the ability to make IFN-γ, the growth delay previously shown between B16/IL-12 compared with B16 in WT mice was not observed (Fig. 4*A*), as was seen in WT mice. When stained for VEGFR3 and quantified by image analysis, both B16 and B16/IL-12 in the IFN-γ$^{-/-}$ mice contained VEGFR3 positive tumor vessels indicating that IFN-γ has an integral role in the suppression of VEGFR3 on tumor vessels (Fig. 4*B*).

IFN-γ–producing T cells are responsible for suppressing VEGFR3

In light of the evidence that IFN-γ is required to suppress VEGFR3, we next assessed the effect of IL-12 on the number of IFN-γ–producing cells within the tumor, particularly T and NK cells, because IL-12 increases IFN-γ production by both (4). To determine the number of IFN-γ–producing TILs, either B16 or B16/IL-12 cells were injected into WT mice, the tumors removed at equivalent thigh diameters, dissociated into single cell suspensions, and the cells pulsed overnight with the melanoma-associated Ag Trp-2, found in B16. The following day, the TILs were stained intracellularly for IFN-γ and analyzed by flow cytometry. In the case of all subsets examined ($CD4^+$, $CD8^+$, and $NK1.1^+$), the number of IFN-γ–producing cells per tumor was significantly higher in B16/IL-12 (Fig. 4*C*). This increase in the number of IFN-γ–producing cells, and the likely increase in intratumoral IFN-γ, could be responsible for the suppression of VEGFR3 on the tumor vessels within B16/IL-12. It has been shown that IFN-γ can suppress the transcription of certain melanoma lineage markers in the melanoma tumor microenvironment (39). To address the possibility that the transcription of VEGFR3 might be suppressed in B16/IL-12, we isolated RNA from whole tumor homogenate of both B16 and B16/IL-12 tumors grown in WT mice. Not only were we able to see a significant decrease in VEGFR3 transcript in B16/IL-12 tumors, but we also saw a concomitant increase in the transcription of IFN-γ as well (data not shown). This reinforces the decrease in VEGFR3 protein we observed in B16/IL-12 tumors by whole mount histology.

To determine whether one or both subsets are required for the downregulation of VEGFR3, B16 and B16/IL-12 were injected into WT mice depleted of NK cells by treatment with an anti-NK1.1 Ab. The treatment protocol used for Ab depletion is indicated in Fig. 5*A* and the absence of NK cells was confirmed by flow cytometry both in the tumor and the spleen at the time of sacrifice (data not shown). In the absence of NK cells, the same tumor suppression is seen in B16/IL-12, as in untreated WT mice (Fig. 1*A* versus Fig. 5*A*). Analysis of the VEGFR3 levels within whole mount samples taken from these tumors confirms that the absence of NK cells does not affect the ability of IL-12–induced IFN-γ to suppress VEGFR3 within B16/IL-12 (Fig. 5*B*).

Because we established that NK cells are not absolutely required to suppress VEGFR3 within B16/IL-12 tumors, we next investigated whether T cells were required to suppress VEGFR3. To accomplish this, we used nude mice that, although lacking T cells, have functional NK cells. These mice were treated with nonspecific rat IgG (Fig. 6*A*) or a rat IgG specific for IL-2Rβ, which effectively depletes NK cells (40) (Fig. 6*B*). In this way, we can compare VEGFR3 suppression in tumors grown in mice that lack T cells and those that lack both T and NK cells to determine whether the IFN-γ produced by tumor-infiltrating NK cells is sufficient to downregulate vascular expression of VEGFR3. Not surprisingly, both B16 and B16/IL-12 grow faster in nude mice (the absence of T cells, but presence of NK cells) than in their WT counterparts. B16/IL-12 still grows more slowly than parental B16 in nude mice, although the extent of tumor control is less than in WT mice (Figs. 1*A*, 6*A*). When both T cells and NK cells are absent, there is no difference in the growth rate between B16 and B16/IL-12 tumors (Fig. 6*B*), which indicates that the tumor control seen in B16/IL-12 can be mediated partially by NK cells in the absence of T cells. On analysis of VEGFR3 levels on the tumor vessels, we found that in the absence of T cells, IL-12 was not able to suppress VEGFR3 on tumor vessels (Fig. 6*C*). Likewise, vessels in both B16 and B16/IL-12 tumors from mice treated with anti–IL-2Rβ, which lack both T cells and NK cells, were unable to suppress VEGFR3 expression (Fig. 6*C*). This indicates that tumor-infiltrating NK cells, in the absence of T cells, are insufficient to effect the suppression of VEGFR3 on the tumor vessel endothelial cells. Taken together, these data demonstrate that T cells are the cell subset responsible for VEGFR3 suppression on B16/IL-12 tumor vessels.

IFN-γ acts on both immune and nonhematopoietic cells to suppress VEGFR3

IFN-γ has been demonstrated necessary to suppress VEGFR3 on tumor vessels (Fig. 4*B*); however, it remains to be seen whether IFN-γ acts directly on the tumor vessels or induces the production of a secondary mediator, which suppresses VEGFR3. To elucidate this mechanism, we generated chimeric mice using IFN-γR$^{-/-}$ mice as the bone marrow donors. Interestingly, we found that when we injected B16/IL-12 into chimeric IFN-γR$^{-/-}$→WT mice, the tumors only grew once the cells had lost their ability to produce IL-12 (data not shown). To eliminate the possibility of direct suppressive effects of IFN-γ on the tumor cells, we instead used tumor lines transfected with the gene for IFN-γR dominant-negative mutant (DNM) (B16/DNM and B16/IL-12/DNM), which would significantly decrease the amount of productive IFN-γ signaling on the tumor cells.

Although in both chimeras we saw a delay in B16/IL-12/DNM growth, as compared with B16/DNM (Fig. 7*A*, 7*B*), surprisingly, we found a larger delay in the B16/IL-12/DNM tumors within the IFN-γR$^{-/-}$→WT mice (Fig. 7*B*). When VEGFR3 was quantified on the tumor vessels, we found that vessels within the IL-12–producing tumors were VEGFR3 negative in both the IFN-γR$^{-/-}$→WT and WT→IFN-γR$^{-/-}$ chimeras. These results indicate that IFN-γ can act directly on the tumor vessel endothelium, or that IFN-γ induces an endothelial cell-produced tertiary mediator that acts in an autocrine fashion to affect the downregulation of VEGR3. However, within mice in which the endothelial cells are unable to respond to IFN-γ, there appears to be a tertiary mediator produced by immune cells in response to intratumoral IFN-γ that can suppress VEGFR3 (Fig. 7*C*).

Discussion

Very little is known of the mechanisms by which the levels of VEGFR3 are regulated on either normal or tumor vessels. In this study, we have shown that IL-12 can suppress the aberrant expression of VEGFR3 on tumor vessels via an IFN-γ–dependent mechanism (Fig. 4*B*). IFN-γ is produced by the TILs and NK cells (Fig. 4*C*); however, it is the T cells that are required for the IL-12–mediated VEGFR3 suppression (Fig. 6). Using IFN-γR$^{-/-}$ bone marrow chimeras, we have found that in the absence of immune cell responsiveness to IFN-γ, VEGFR3 can still be suppressed via a direct mechanism of IFN-γ acting on vessel endothelial cells (Fig. 7). Interestingly, IFN-γ can also act in an indirect mechanism in animals that have endothelial cells unable to respond to IFN-γ. There exists the possibility that a small population of mesenchymal stem cells may have been transferred with the donor marrow that could result in the presence of fibroblasts and endothelial cells of donor origin that could have a role in the antiangiogenesis in these tumors (41). To examine this, we grew tumors in chimeric mice in which WT recipients received GFP^{+} bone marrow. Flow cytometry revealed a subset of tumor-associated GFP^{+} cells; however, the vast majority (>95%) of these cells were CD45^{+} and therefore not fibroblasts. In addition, we failed to observe any GFP^{+} tumor vessels (data not shown). Therefore, we have no evidence to suggest that donor bone marrow can develop into significant numbers of either stromal or endothelial cells within our model. Thus, there appears to be at least two distinct mechanisms by which IFN-γ can suppress VEGFR3.

The indirect mechanism by which IFN-γ can downregulate VEGFR3 requires an immune cell-produced mediator. The candidate for this mediator could be any gene product that is downstream of IFN-γ signaling that can act on endothelial cells. The chemokine CXCL10 is one of the few mediators for which there is published data for a role in the antiangiogenic axis initiated by IL-12. For example, it has been reported that blocking CXCL10 abrogates the antiangiogenic effects of IL-12 within IL-12–treated tumors (42,43). Thus, CXCL10 is a likely potential mediator of the indirect mechanism of IFN-γ on tumor vessel endothelial cells. To test the role of CXCL10 and other ligands of CXCR3, we injected B16 and B16/

IL-12 into CXCR3$^{-/-}$ mice. In these experiments, even in the absence of CXCR3 signaling, IL-12 was still able to downregulate VEGFR3 on the tumor vessels (data not shown), suggesting that the ligands of CXCR3, including CXCL10, are not essential for the suppression of VEGFR3. This is in line with our findings that, even when the indirect mechanism is blocked, IFN-γ can act directly on endothelial cells to down-regulate VEGFR3.

Regarding the direct mechanism of IFN-γ–mediated VEGFR3 suppression, it is possible that IFN-γ acts alone on tumor endothelial cells to suppress VEGFR3 by upregulating receptors known to suppress VEGFR3. Recent studies into VEGFR3 regulation have revealed a role for the Notch ligand Delta-like 4 (DLL4) and Notch1 in antiangiogenesis and VEGFR3 downregulation. Interestingly, although VEGF is a strongly proangiogenic factor, it has recently been shown to induce DLL4 in tip cells, the single specialized endothelial cell at the leading edge of a vessel sprout that can define the direction in which the newly formed vessel grows or if it grows at all. The upregulation of DLL4 in tip cells in turn suppresses sprouting in the adjacent endothelial cells through its interaction with Notch1 (44-47). Interestingly, Notch signaling can suppress VEGFR3 on the surface of tumor vessels (34). Therefore, it is possible that IFN-γ acts via endothelial Notch1 regulation; indeed, preliminary experiments in vitro, using an immortalized mouse endothelial cell line (SVEC), have indicated that IFN-γ can upregulate Notch1 mRNA in a CXCL10-independent fashion (data not shown). If IFN-γ has a role in the downregulation of endothelial Notch1, it could be responsible for the direct mechanism of IFN-γ–mediated VEGFR3 downregulation.

Vessels within tumors are known to be chaotic and poorly formed; however, the presence of IL-12 seems to have a normalizing effect on tumor vasculature morphology, as shown by a decrease in the number and the diameter of the tumor vessels, as well as a suppression of VEGFR3 (20). The suppression of VEGFR3 on tumor vessels can improve tumor control in several ways. It may increase the efficacy of current angiogenic treatments such as Avastin (Genentech, San Francisco, CA). Because this treatment only blocks VEGF-A, and many types of tumors contain vessels that express VEGFR3, VEGF-C and VEGF-D within the tumor can continue to act in a proangiogenic manner. Indeed, even in the absence of VEGF-A, VEGFR2 can enhance VEGFR3 phosphorylation and signaling by heterodimerizing with it (48,49). In addition, the outright blockade of VEGFR3 alone within the tumor results in decreased vessel formation and increased tumor control (28,29). Aside from the positive effects yielded from VEGFR3 suppression alone, it is thought that overall vascular normalization could possibly lead to more potent tumor control. For example, blockade of VEGF leads to less leaky and dilated vessels, and increases pericyte coverage (18). Therefore, although both anti-angiogenic therapies and local treatment of tumors with IL-12 cause a decrease in the number of vessels and may lead to more areas of hypoxia, the vessels that remain become more functional as they normalize. Although fewer in number, these normalized vessels could increase drug delivery to the tumor and may enhance lymphocyte function through relieving hypoxia, a condition that can suppress immune function in multiple ways. For example, hypoxia can decrease production of T cell prosurvival and procytotoxic cytokines (IL-2 and IFN-γ) and an induction of cAMP, which can interfere with the effector signaling pathways (50,51). In addition, elevated tumor oxygenation can increase efficacy of radiation therapy because of the increase of oxygenation of the tumor cells themselves.

The concept of using the immune system to alter the vasculature is a novel one. Thus, promoting immunotherapy may have 2-fold effects of: 1) enhancing the immune response to recognize and eliminate tumor cells, and 2) suppressing angiogenesis, which not only slows tumor growth, but may also normalize vessels resulting in increased influx of immune cells,

which will continue to have antiangiogenic effects on the vasculature. This cyclic process may result in potent antitumor effects.

Acknowledgments

This work was supported by National Institutes of Health Grant CA28332. E.W.S. was supported by the National Institutes of Health Training Grant AI007285.

Abbreviations used in this paper

DLL4	Delta-like 4
DNM	dominant-negative mutant
TIL	tumor infiltrating lymphocyte
VEGF	vascular endothelial growth factor
VEGFR3	VEGF receptor 3
WT	wild-type.

References

1. Rosenberg SA, Lotze MT, Yang JC, Linehan WM, Seipp C, Calabro S, Karp SE, Sherry RM, Steinberg S, White DE. Combination therapy with interleukin-2 and alpha-interferon for the treatment of patients with advanced cancer. J. Clin. Oncol. 1989; 7:1863–1874. [PubMed: 2685181]
2. Dorval T, Mathiot C, Chosidow O, Revuz J, Avril MF, Guillaume JC, Tursz T, Brandely M, Pouillart P, Fridman WH. IL-2 phase II trial in metastatic melanoma: analysis of clinical and immunological parameters. Biotechnol. Ther. 1992; 3:63–79. [PubMed: 1305893]
3. Margolin KA, Doroshow JH, Akman SA, Leong LA, Morgan RJ, Raschko J, Somlo G, Mills B, Goldberg D, Sniecinski I. 1992. Phase I trial of interleukin-2 plus gamma-interferon. J. Immunother. 1991; 11:50–55. [PubMed: 1734948]
4. Brunda MJ. Interleukin-12. J. Leukoc. Biol. 1994; 55:280–288. [PubMed: 7905508]
5. Trinchieri G, Scott P. The role of interleukin 12 in the immune response, disease and therapy. Immunol. Today. 1994; 15:460–463. [PubMed: 7945769]
6. Banks RE, Patel PM, Selby PJ. Interleukin 12: a new clinical player in cytokine therapy. Br. J. Cancer. 1995; 71:655–659. [PubMed: 7710924]
7. Croft M, Carter L, Swain SL, Dutton RW. Generation of polarized antigen-specific CD8 effector populations: reciprocal action of interleukin (IL)-4 and IL-12 in promoting type 2 versus type 1 cytokine profiles. J. Exp. Med. 1994; 180:1715–1728. [PubMed: 7525836]
8. Hess SD, Egilmez NK, Bailey N, Anderson TM, Mathiowitz E, Bernstein SH, Bankert RB. Human CD4+ T cells present within the microenvironment of human lung tumors are mobilized by the local and sustained release of IL-12 to kill tumors in situ by indirect effects of IFN-gamma. J. Immunol. 2003; 170:400–412. [PubMed: 12496425]
9. Zou JP, Yamamoto N, Fujii T, Takenaka H, Kobayashi M, Herrmann SH, Wolf SF, Fujiwara H, Hamaoka T. Systemic administration of rIL-12 induces complete tumor regression and protective immunity: response is correlated with a striking reversal of suppressed IFN-γamma production by anti-tumor T cells. Int. Immunol. 1995; 7:1135–1145. [PubMed: 8527411]
10. Ogawa M, Tsutsui T, Zou JP, Mu J, Wijesuriya R, Yu WG, Herrmann S, Kubo T, Fujiwara H, Hamaoka T. Enhanced induction of very late antigen 4/lymphocyte function-associated antigen 1-dependent T-cell migration to tumor sites following administration of interleukin 12. Cancer Res. 1997; 57:2216–2222. [PubMed: 9187124]
11. Atkins MB, Robertson MJ, Gordon M, Lotze MT, DeCoste M, DuBois JS, Ritz J, Sandler AB, Edington HD, Garzone PD, et al. Phase I evaluation of intravenous recombinant human interleukin 12 in patients with advanced malignancies. Clin. Cancer Res. 1997; 3:409–417. [PubMed: 9815699]

12. Gollob JA, Mier JW, Veenstra K, McDermott DF, Clancy D, Clancy M, Atkins MB. Phase I trial of twice-weekly intravenous interleukin 12 in patients with metastatic renal cell cancer or malignant melanoma: ability to maintain IFN-γamma induction is associated with clinical response. Clin. Cancer Res. 2000; 6:1678–1692. [PubMed: 10815886]

13. Gollob JA, Mier JW, Atkins MB. Clinical use of systemic IL-12 therapy. Cancer Chemother. Biol. Response Modif. 2001; 19:353–369. [PubMed: 11686023]

14. Brunda MJ, Luistro L, Warrier RR, Wright RB, Hubbard BR, Murphy M, Wolf SF, Gately MK. Antitumor and antimetastatic activity of interleukin 12 against murine tumors. J. Exp. Med. 1993; 178:1223–1230. [PubMed: 8104230]

15. Nastala CL, Edington HD, McKinney TG, Tahara H, Nalesnik MA, Brunda MJ, Gately MK, Wolf SF, Schreiber RD, Storkus WJ, et al. Recombinant IL-12 administration induces tumor regression in association with IFN-γamma production. J. Immunol. 1994; 153:1697–1706. [PubMed: 7913943]

16. Dias S, Boyd R, Balkwill F. IL-12 regulates VEGF and MMPs in a murine breast cancer model. Int. J. Cancer. 1998; 78:361–365. [PubMed: 9766572]

17. Moran JP, Gerber SA, Martin CA, Frelinger JG, Lord EM. Transfection of the genes for interleukin-12 into the K1735 melanoma and the EMT6 mammary sarcoma murine cell lines reveals distinct mechanisms of antitumor activity. Int. J. Cancer. 2003; 106:690–698. [PubMed: 12866028]

18. Jain RK. Normalization of tumor vasculature: an emerging concept in antiangiogenic therapy. Science. 2005; 307:58–62. [PubMed: 15637262]

19. Nakahara T, Norberg SM, Shalinsky DR, Hu-Lowe DD, McDonald DM. Effect of inhibition of vascular endothelial growth factor signaling on distribution of extravasated antibodies in tumors. Cancer Res. 2006; 66:1434–1445. [PubMed: 16452199]

20. Gerber SA, Moran JP, Frelinger JG, Frelinger JA, Fenton BM, Lord EM. Mechanism of IL-12 mediated alterations in tumour blood vessel morphology: analysis using whole-tissue mounts. Br. J. Cancer. 2003; 88:1453–1461. [PubMed: 12778077]

21. Dumont DJ, Jussila L, Taipale J, Lymboussaki A, Mustonen T, Pajusola K, Breitman M, Alitalo K. Cardiovascular failure in mouse embryos deficient in VEGF receptor-3. Science. 1998; 282:946–949. [PubMed: 9794766]

22. Kaipainen A, Korhonen J, Mustonen T, van Hinsbergh VW, Fang GH, Dumont D, Breitman M, Alitalo K. Expression of the fms-like tyrosine kinase 4 gene becomes restricted to lymphatic endothelium during development. Proc. Natl. Acad. Sci. USA. 1995; 92:3566–3570. [PubMed: 7724599]

23. Paavonen K, Puolakkainen P, Jussila L, Jahkola T, Alitalo K. Vascular endothelial growth factor receptor-3 in lymphangiogenesis in wound healing. Am. J. Pathol. 2000; 156:1499–1504. [PubMed: 10793061]

24. Clarijs R, Schalkwijk L, Hofmann UB, Ruiter DJ, de Waal RM. Induction of vascular endothelial growth factor receptor-3 expression on tumor microvasculature as a new progression marker in human cutaneous melanoma. Cancer Res. 2002; 62:7059–7065. [PubMed: 12460927]

25. Valtola R, Salven P, Heikkilä P, Taipale J, Joensuu H, Rehn M, Pihlajaniemi T, Weich H, deWaal R, Alitalo K. VEGFR-3 and its ligand VEGF-C are associated with angiogenesis in breast cancer. Am. J. Pathol. 1999; 154:1381–1390. [PubMed: 10329591]

26. Partanen TA, Alitalo K, Miettinen M. Lack of lymphatic vascular specificity of vascular endothelial growth factor receptor 3 in 185 vascular tumors. Cancer. 1999; 86:2406–2412. [PubMed: 10590384]

27. Filho, A. Longatto; Martins, A.; Costa, SM.; Schmitt, FC. VEGFR-3 expression in breast cancer tissue is not restricted to lymphatic vessels. Pathol. Res. Pract. 2005; 201:93–99. [PubMed: 15901129]

28. Kubo H, Fujiwara T, Jussila L, Hashi H, Ogawa M, Shimizu K, Awane M, Sakai Y, Takabayashi A, Alitalo K, et al. Involvement of vascular endothelial growth factor receptor-3 in maintenance of integrity of endothelial cell lining during tumor angiogenesis. Blood. 2000; 96:546–553. [PubMed: 10887117]

29. Laakkonen P, Waltari M, Holopainen T, Takahashi T, Pytowski B, Steiner P, Hicklin D, Persaud K, Tonra JR, Witte L, Alitalo K. Vascular endothelial growth factor receptor 3 is involved in tumor angiogenesis and growth. Cancer Res. 2007; 67:593–599. [PubMed: 17234768]
30. Jeltsch M, Kaipainen A, Joukov V, Meng X, Lakso M, Rauvala H, Swartz M, Fukumura D, Jain RK, Alitalo K. Hyperplasia of lymphatic vessels in VEGF-C transgenic mice. Science. 1997; 276:1423–1425. [PubMed: 9162011]
31. Oh SJ, Jeltsch MM, Birkenhäger R, McCarthy JE, Weich HA, Christ B, Alitalo K, Wilting J. VEGF and VEGF-C: specific induction of angiogenesis and lymphangiogenesis in the differentiated avian chorioallantoic membrane. Dev. Biol. 1997; 188:96–109. [PubMed: 9245515]
32. Cao Y, Linden P, Farnebo J, Cao R, Eriksson A, Kumar V, Qi JH, Claesson-Welsh L, Alitalo K. Vascular endothelial growth factor C induces angiogenesis in vivo. Proc. Natl. Acad. Sci. USA. 1998; 95:14389–14394. [PubMed: 9826710]
33. Witmer AN, van Blijswijk BC, Dai J, Hofman P, Partanen TA, Vrensen GF, Schlingemann RO. VEGFR-3 in adult angiogenesis. J. Pathol. 2001; 195:490–497. [PubMed: 11745682]
34. Tammela T, Zarkada G, Wallgard E, Murtomäki A, Suchting S, Wirzenius M, Waltari M, Hellström M, Schomber T, Peltonen R, et al. Blocking VEGFR-3 suppresses angiogenic sprouting and vascular network formation. Nature. 2008; 454:656–660. [PubMed: 18594512]
35. Wu YP, McMahon E, Kraine MR, Tisch R, Meyers A, Frelinger J, Matsushima GK, Suzuki K. Distribution and characterization of GFP(+) donor hematogenous cells in Twitcher mice after bone marrow transplantation. Am. J. Pathol. 2000; 156:1849–1854. [PubMed: 10854208]
36. McAdam AJ, Pulaski BA, Storozynsky E, Yeh KY, Sickel JZ, Frelinger JG, Lord EM. Analysis of the effect of cytokines (interleukins 2, 3, 4, and 6, granulocyte-monocyte colony-stimulating factor, and interferon-gamma) on generation of primary cytotoxic T lymphocytes against a weakly immunogenic tumor. Cell. Immunol. 1995; 165:183–192. [PubMed: 7553882]
37. Blieden TM, McAdam AJ, Frelinger JG, Lord EM. Mechanism of cytolytic T lymphocyte killing of a low class I-expressing tumor. J. Immunol. 1991; 147:1433–1438. [PubMed: 1907998]
38. Tanaka T, Tsudo M, Karasuyama H, Kitamura F, Kono T, Hatakeyama M, Taniguchi T, Miyasaka M. A novel monoclonal antibody against murine IL-2 receptor beta-chain. Characterization of receptor expression in normal lymphoid cells and EL-4 cells. J. Immunol. 1991; 147:2222–2228. [PubMed: 1918958]
39. Meije CB, Swart GW, Lepoole C, Das PK, Van den Oord JJ. Antigenic profiles of individual-matched pairs of primary and melanoma metastases. Hum. Pathol. 2009; 40:1399–1407. [PubMed: 19386352]
40. Ehl S, Nuesch R, Tanaka T, Myasaka M, Hengartner H, Zinkernagel R. A comparison of efficacy and specificity of three NK depleting antibodies. J. Immunol. Methods. 1996; 199:149–153. [PubMed: 8982356]
41. Lu Y, Yang W, Qin C, Zhang L, Deng J, Liu S, Qin Z. Responsiveness of stromal fibroblasts to IFN-gamma blocks tumor growth via angiostasis. J. Immunol. 2009; 183:6413–6421. [PubMed: 19841170]
42. Coughlin CM, Salhany KE, Gee MS, LaTemple DC, Kotenko S, Ma X, Gri G, Wysocka M, Kim JE, Liu L, et al. Tumor cell responses to IFNgamma affect tumorigenicity and response to IL-12 therapy and antiangiogenesis. Immunity. 1998; 9:25–34. [PubMed: 9697833]
43. Sgadari C, Angiolillo AL, Tosato G. Inhibition of angiogenesis by interleukin-12 is mediated by the interferon-inducible protein 10. Blood. 1996; 87:3877–3882. [PubMed: 8611715]
44. Noguera-Troise I, Daly C, Papadopoulos NJ, Coetzee S, Boland P, Gale NW, Lin HC, Yancopoulos GD, Thurston G. Blockade of Dll4 inhibits tumour growth by promoting non-productive angiogenesis. Nature. 2006; 444:1032–1037. [PubMed: 17183313]
45. Ridgway J, Zhang G, Wu Y, Stawicki S, Liang WC, Chanthery Y, Kowalski J, Watts RJ, Callahan C, Kasman I, et al. Inhibition of Dll4 signalling inhibits tumour growth by deregulating angiogenesis. Nature. 2006; 444:1083–1087. [PubMed: 17183323]
46. Lobov IB, Renard RA, Papadopoulos N, Gale NW, Thurston G, Yancopoulos GD, Wiegand SJ. Delta-like ligand 4 (Dll4) is induced by VEGF as a negative regulator of angiogenic sprouting. Proc. Natl. Acad. Sci. USA. 2007; 104:3219–3224. [PubMed: 17296940]

47. Suchting S, Freitas C, le Noble F, Benedito R, Bréant C, Duarte A, Eichmann A. The Notch ligand Delta-like 4 negatively regulates endothelial tip cell formation and vessel branching. Proc. Natl. Acad. Sci. USA. 2007; 104:3225–3230. [PubMed: 17296941]

48. Alam A, Herault JP, Barron P, Favier B, Fons P, Delesque-Touchard N, Senegas I, Laboudie P, Bonnin J, Cassan C, et al. Heterodimerization with vascular endothelial growth factor receptor-2 (VEGFR-2) is necessary for VEGFR-3 activity. Biochem. Biophys. Res. Commun. 2004; 324:909–915. [PubMed: 15474514]

49. Hamada K, Oike Y, Takakura N, Ito Y, Jussila L, Dumont DJ, Alitalo K, Suda T. VEGF-C signaling pathways through VEGFR-2 and VEGFR-3 in vasculoangiogenesis and hematopoiesis. Blood. 2000; 96:3793–3800. [PubMed: 11090062]

50. Kim H, Peng G, Hicks JM, Weiss HL, Van Meir EG, Brenner MK, Yotnda P. Engineering human tumor-specific cytotoxic T cells to function in a hypoxic environment. Mol. Ther. 2008; 16:599–606. [PubMed: 18227840]

51. Sitkovsky MV. Use of the A(2A) adenosine receptor as a physiological immunosuppressor and to engineer inflammation in vivo. Biochem. Pharmacol. 2003; 65:493–501. [PubMed: 12566076]

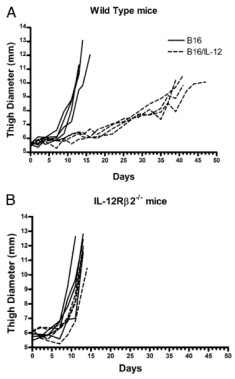

FIGURE 1.

Local production of IL-12 delays growth of B16. B16 (solid lines) or B16/IL-12 (dotted lines) cells (2×10^5) were injected i.m. into (*A*) WT or (*B*) IL-12Rβ2$^{-/-}$ mice and the thigh diameter measured over time. Each line represents one mouse. Growth curves are representative plots from two independent experiments.

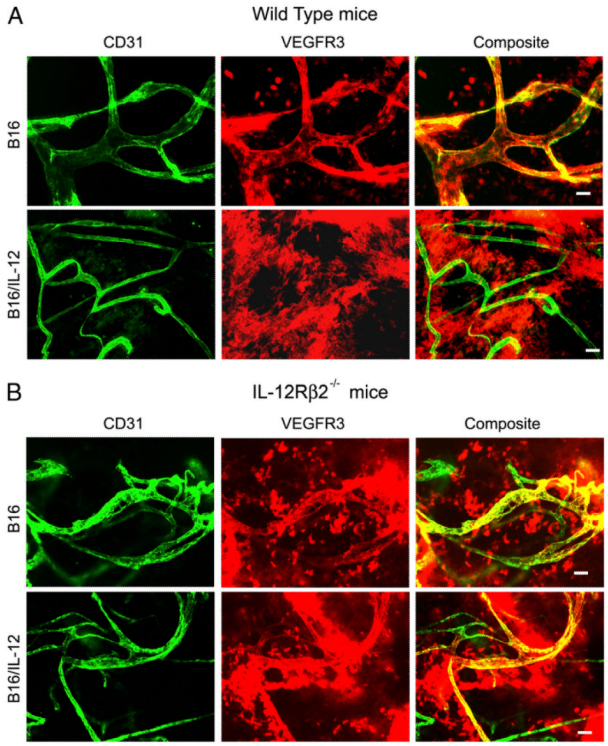

FIGURE 2.

IL-12 suppresses VEGFR3 on tumor vessels. B16 or B16/IL-12 cells (2×10^5) were injected i.m. into (*A*) WT or (*B*) IL-12Rβ2$^{-/-}$ mice and grown to a mean thigh diameter of 10–13 mm. Representative images of whole mount preparations of B16 (*top rows*) and B16/IL-12 (*bottom rows*) are shown stained with biotinylated anti-VEGFR3 and PE-streptavidin (pseudo-colored red) and FITC-conjugated anti-CD31 (pseudo-colored green). Scale bar, 50 μm.

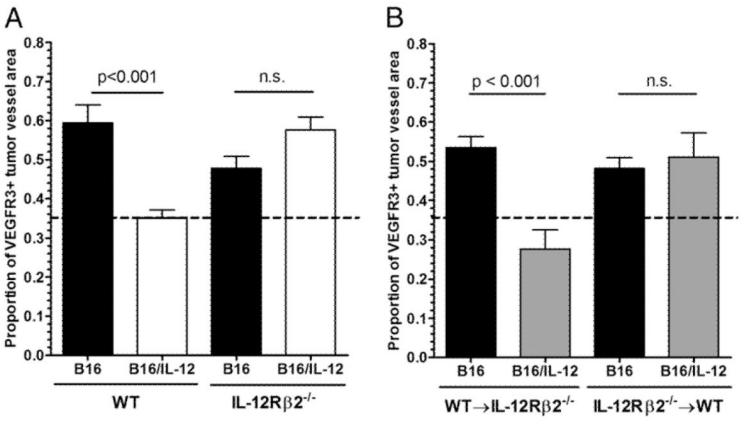

FIGURE 3.

IL-12 does not act directly on endothelial cells or tumor cells to mediate VEGFR3 suppression on tumor vessels. *A*, B16 or B16/IL-12 cells (2×10^5) were injected i.m. into WT or IL-12Rβ2$^{-/-}$ mice and grown to a mean thigh diameter of 10–13 mm. *B*, Lethally irradiated WT or IL-12Rβ2$^{-/-}$ mice were reconstituted with WT or IL-12Rβ2$^{-/-}$ bone marrow, rested for 8 wk, and injected i.m. with 2×10^5 B16 or B16/IL-12 cells. Tumors were then removed as stated in the *Materials and Methods*, stained for VEGFR3 and CD31, and visualized by whole mount fluorescence microscopy. The proportion of vessel area that stained positive for VEGFR3 was calculated using ImagePro software. The dotted line at 0.36 represents the level of staining seen in B16/IL-12 tumors grown in a WT mouse, which does not have VEGFR3 on its vessels and therefore represents nonspecific staining. Graphs represent two experiments with four to six animals per condition. Significance was calculated using Bonferroni's multiple comparison test.

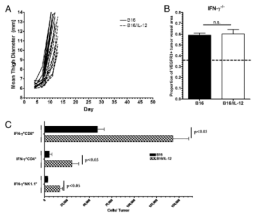

FIGURE 4.

IL-12 suppresses VEGFR3 on tumor vessels via IFN-γ and upregulates IFN-γ production by tumor infiltrating immune cells. *A*, B16 (solid lines) or B16/IL-12 (dotted lines) cells (2×10^5) were injected i.m. into IFN-$\gamma^{-/-}$ mice and thigh diameter measured over time. Each line represents one mouse. *B*, The proportion of vessel area that stained positive for VEGFR3 in the mice described in *A* was calculated using ImagePro software. The dotted line at 0.36 represents the level of staining seen in B16/IL-12 tumors grown in a WT mouse, which does not have VEGFR3 on its vessels and therefore represents nonspecific staining. Growth curves and VEGFR3 quantification represents pooled data from two experiments with a total of six animals per group. *C*, WT mice injected with 2×10^5 B16 or B16/IL-12 cells. Tumors were grown to a thigh diameter of 10 mm, weight-matched, and analyzed for IFN-γ production by intracellular cytokine staining. Each population was pregated on $CD45^+$ cells. Significance was calculated using Mann-Whitney *U* test.

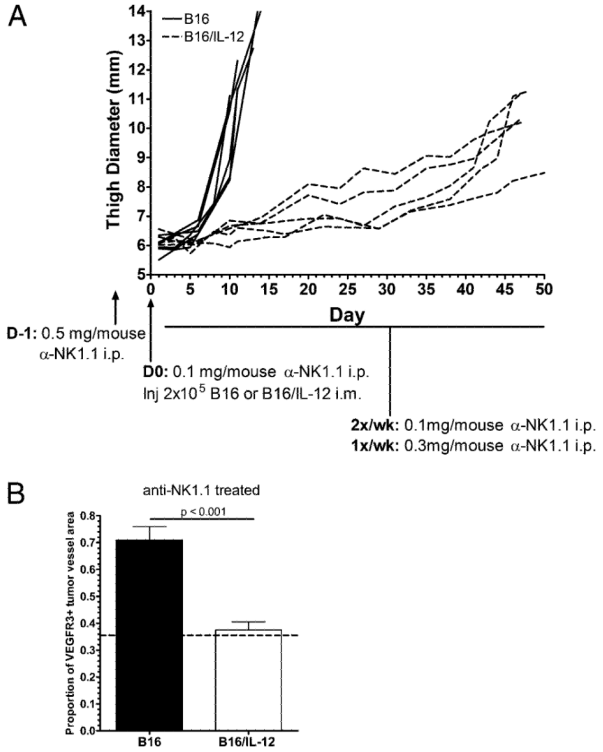

FIGURE 5.

T cells are sufficient to suppress VEGFR3. C57BL/6 mice were treated with anti-NK1.1 IgG. *A*, B16 (solid lines) or B16/IL-12 (dotted lines) cells (2×10^5) were injected i.m. and thigh diameter measured over time. Each line represents one mouse. *B*, Tumors were then removed and stained with biotinylated anti-VEGFR3 and PE-streptavidin and allophycocyanin-conjugated anti-CD31 and visualized by whole mount fluorescence microscopy. The dotted line at 0.36 represents the level of staining seen in B16/IL-12 tumors grown in a WT mouse, which does not have VEGFR3 on its vessels and therefore represents nonspecific staining. Growth curves are representative plots and VEGFR3 quantification represents pooled data from two experiments with a total of five to seven animals per group. Significance was calculated using Mann-Whitney *U* test.

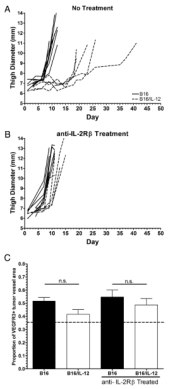

FIGURE 6.

NK cells are insufficient to suppress VEGFR3 in the absence of T cells. Nude mice were (*A*) left untreated or (*B*) treated with anti–IL-2Rβ IgG. B16 (solid lines) or B16/IL-12 (dotted lines) cells (2×10^5) were injected i.m. and thigh diameter measured over time. Each line represents one mouse. *C*, Tumors were then removed and stained with biotinylated anti-VEGFR3 and PE-streptavidin and allophycocyanin-conjugated anti-CD31 and visualized by whole mount fluorescence microscopy. The dotted line at 0.36 represents the level of staining seen in B16/IL-12 tumors grown in a WT mouse, which does not have VEGFR3 on its vessels and therefore represents nonspecific staining. Growth curves are representative plots and VEGFR3 quantification represents pooled data from two experiments with a total of five to seven animals per group. Significance was calculated using Bonferroni's multiple comparison test.

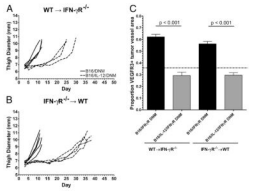

FIGURE 7.

IFN-γ indirectly suppresses VEGFR3 on tumor vasculature. Lethally irradiated IFN-γR$^{-/-}$ or WT mice were reconstituted with (*A*) WT or (*B*) IFN-γR$^{-/-}$ bone marrow, respectively, rested for 8 wk, and injected i.m. with 2 × 10^5 B16/IFN-γR DNM (B16/DNM, solid lines) or B16/IL-12/DNM (dashed lines) cells. Mean thigh diameter was measured over time and the tumors were grown to a mean thigh diameter of 10–12 mm before use. Each line represents one mouse. *C*, Tumors were then removed and stained for VEGFR3 and CD31 and visualized by whole mount fluorescence microscopy. The proportion of vessel area that stained positive for VEGFR3 was calculated using ImagePro software. The dotted line at 0.36 represents the level of staining seen in B16/IL-12 tumors grown in a WT mouse, which does not have VEGFR3 on its vessels and therefore represents nonspecific staining. Graphs represent two experiments with four to six animals per condition. Significance was calculated using Bonferroni's multiple comparison test.